LETTER

Progressive incision of the Channeled Scablands by outburst floods

Isaac J. Larsen[1,2] & Michael P. Lamb[2]

The surfaces of Earth and Mars contain large bedrock canyons that were carved by catastrophic outburst floods[1,2]. Reconstructing the magnitude of these canyon-forming floods is essential for understanding the ways in which floods modify planetary surfaces[1,2], the hydrology of early Mars[3] and abrupt changes in climate[4]. Flood discharges are often estimated by assuming that the floods filled the canyons to their brims with water; however, an alternative hypothesis is that canyon morphology adjusts during incision such that bed shear stresses exceed the threshold for erosion by a small amount[5]. Here we show that accounting for erosion thresholds during canyon incision results in near-constant discharges that are five- to ten-fold smaller than full-to-the-brim estimates for Moses Coulee, a canyon in the Channeled Scablands, which was carved during the Pleistocene by the catastrophic Missoula floods in eastern Washington, USA. The predicted discharges are consistent with flow-depth indicators from gravel bars within the canyon. In contrast, under the assumption that floods filled canyons to their brims, a large and monotonic increase in flood discharge is predicted as the canyon was progressively incised, which is at odds with the discharges expected for floods originating from glacial lake outbursts. These findings suggest that flood-carved landscapes in fractured rock might evolve to a threshold state for bedrock erosion, thus implying much lower flood discharges than previously thought.

Field investigation of the Channeled Scablands, which contains vast tracts of scoured bedrock, giant gravel bars and deep canyons, led to the eventual recognition that short-lived, catastrophic floods, rather than uniformitarian processes, were the dominant agents of canyon formation in the region[1,6]. Outburst floods caused by the sudden drainage of lakes due to the failure of glacial or other natural dams have been documented in many settings on Earth[7]; and enormous bedrock canyons, morphologically similar to those in the Channeled Scablands, provide evidence for widespread outburst flooding on the surface of Mars[2]. Canyons carved into planetary surfaces are hence a key record of the palaeo-hydrosphere[3], and constraining the magnitude of the canyon-carving floods is required to understand whether megafloods—immense, short-lived, catastrophic floods—have the potential to trigger climate change, by altering ocean circulation on Earth[4] or by episodically generating oceans on Mars[8].

Although bedrock canyons and associated depositional landforms provide direct evidence for palaeo-floods, reconstructing the hydraulics of outburst floods is challenging. Outburst floods often initiate subglacially[9] or, in the case of Mars, from subsurface aquifers[10]; hence, canyon geometry and the grain size of flood-transported sediment often provide the only clues from which water depth, bed shear stress and discharge can be reconstructed. Outburst floods in the Channeled Scablands and on Mars have traditionally been assumed to fill the canyons up to the elevation of high-water marks such as eroded channel margins[11] along the rims of the canyons. Consequently, most hydraulic modelling efforts implicitly assume that the canyons were filled with water to their brims[11–14] or attempt to match modelled flood depths to the brim-full markers[12,14,15]. However, the actual flow depth is unknown[10] because canyon floors must have progressively lowered as a result of bedrock incision, and high-water markers may have been active only early in canyon formation; therefore, the discharges predicted from 'brim-full' models are reported as maximum estimates[11,13].

In the case of other bedrock canyons that formed over millions of years, such as the Grand Canyon, USA, water flows that were responsible for carving the canyon had depths that were always a small fraction of the canyon relief. Recent mechanistic studies[5,9,16–20] and theory for bedrock erosion by plucking of blocks from the bed[21] or toppling at waterfalls[22,23] indicate that, where rock is fractured, bedrock channels will incise via the entrainment of bedrock blocks from the bed when fluid stresses exceed the threshold for entrainment. This 'threshold shear stress' model implies that flows in outburst-flood-carved canyons will drop below brim-full as canyons deepen. Resolving whether canyons carved by outburst floods should be interpreted as channels filled to the brim or as valleys with flow only near their bottoms is key for reconstructing palaeo-flood discharge. However, evaluating these two 'end-member' models is challenging; both require removal of rock, but information on how canyons evolve during formation is lacking.

We conduct a quantitative evaluation of the end-member brim-full and threshold shear stress models by numerically simulating floods in Moses Coulee, a 70-km-long canyon in the Channeled Scablands (Fig. 1) with evidence of flooding 175 m above the canyon floor and a history of at least four late-Pleistocene-epoch outburst floods[24]. We selected Moses Coulee for the study because, unlike other canyons in the Channeled Scablands, the planform geometry is relatively simple and a set of bedrock terraces enables reconstruction of the palaeo-channel bed during canyon incision. Plucking is the dominant erosion mechanism in the well-jointed basalt bedrock of the Channeled Scablands[6]; however, forward-modelling the co-evolution of hydraulics and bed topography in a megaflood channel that is eroding by plucking is currently intractable, owing to computational expense and the fact that the physics of wall and bed erosion are not well known[21]. Instead, we conducted simulations for the modern Moses Coulee topography and explored how flooding evolved in concert with canyon incision by routeing floods through four inferred stages of canyon formation (Fig. 1c), for which we reconstructed palaeo-topography guided by bedrock terraces (see Methods). Floods were simulated in discharge increments of $0.1 \times 10^6\,\mathrm{m^3\,s^{-1}}$ using a two-dimensional, depth-averaged, hydraulic model. The elevations of high-water marks identified in the field were used to constrain the discharges predicted by the brim-full model. The discharges predicted by the threshold shear stress model were determined from simulations in which bed stresses only slightly exceeded the threshold for incision via bedrock-block plucking, with lower-bound estimates based on the assumption of cohesionless blocks and upper-bound estimates that include interlocking via the inclusion of block wall friction.

[1]Department of Geosciences, University of Massachusetts, Amherst, Massachusetts 01003, USA. [2]Division of Geological and Planetary Sciences, California Institute of Technology, Pasadena, California 91125, USA.
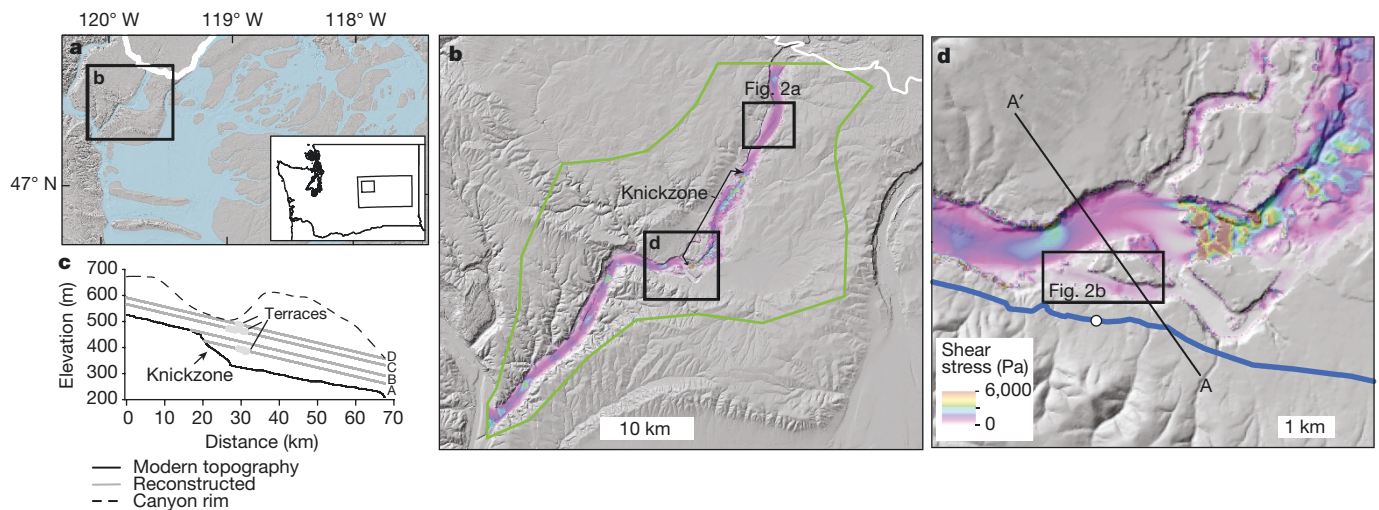
Figure 1 | The Moses Coulee study site. a, Moses Coulee in eastern Washington, USA (location indicated by the smaller boxed region in the inset). Blue areas were inundated by late-Pleistocene floods and the white line delineates the southern extent of the Cordilleran ice sheet. Flood and ice extent are interpreted from version 3.0 of the Washington Department of Natural Resources digital 1:250,000 scale state geological map. **b**, Moses Coulee with modelled bed shear stresses (see colour scale in **d**) during a flood with a discharge of $0.6 \times 10^6\,\mathrm{m^3\,s^{-1}}$; the model domain is outlined in green. **c**, Long profile of Moses Coulee showing the modern bed topography (solid black line), mapped bedrock terraces (grey circles) and the bed topography reconstructed from the terrace elevations (grey lines labelled A–D). The rim of the canyon is indicated by the dashed black line. Elevation is with respect to sea level. **d**, The study reach. The white circle shows the location of the field-defined high-water mark; the blue line shows the high-water line interpreted from aerial imagery. The line A–A′ shows the location of the cross-section in Fig. 4.

The threshold shear stress model for bedrock canyons stems from theoretical and field evidence from gravel-bedded rivers that demonstrates that, on average, bed shear stresses can exceed the threshold for sediment transport by only 20% before the channel cross-section will erode and evolve to a form that maintains shear stresses near the threshold for sediment transport[25]. Hence, well-jointed rock that is subject to megaflooding may behave more like a bed of sediment with limited or no cohesion in which individual blocks can be easily entrained and transported, rather than as massive crystalline rock that erodes slowly through abrasion[5,22,23]. Such bedrock channels cannot withstand large discharges or shear stresses that greatly exceed the threshold for plucking. Instead, the channels will adjust their morphology through bedrock erosion so that bed stresses, on average, only slightly exceed the threshold for block erosion.

The discharges predicted by the two models are tested by assessing the temporal evolution of discharge during canyon incision, because

the brim-full model implies a temporal increase in discharge to maintain brim-full flow while the canyon floor erodes. However, in the Channeled Scablands, at least tens of floods are thought to have occurred[24], and all but the most recent floods probably had comparable discharges, owing to a triggering mechanism that required filling an ice-dammed lake to a threshold level sufficient to float the dam and release an outburst[24]. A second test uses the depositional bars within Moses Coulee, because these require certain levels of inundation and sediment transport regimes to form[26], by determining which model predictions are most consistent with the location and morphology of two key landforms: the Great Gravel Bar (Fig. 2a) and a boulder bar on an 'abandoned channel', a terrace 70 m above the canyon floor (Fig. 2b, c).

The discharge predicted by the brim-full model increases from $0.1 \times 10^6\,\mathrm{m^3\,s^{-1}}$ to a peak of $3.0 \times 10^6\,\mathrm{m^3\,s^{-1}}$ (Fig. 3a) during canyon formation; the peak discharge value during the final stage of canyon
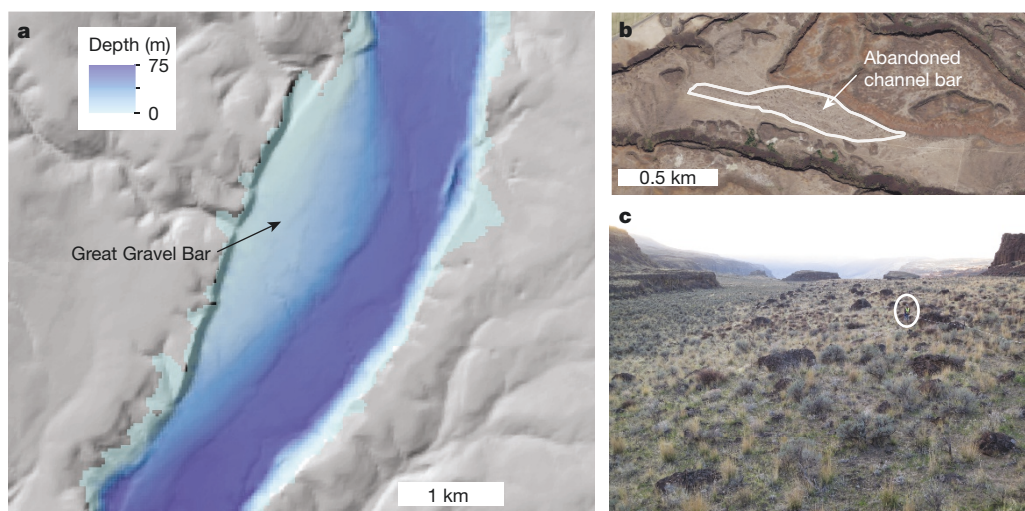
Figure 2 | Depositional landforms in Moses Coulee. a, The Great Gravel Bar in upper Moses Coulee overlain by a water-depth map for a simulated flood with a discharge of $0.6 \times 10^6\,\mathrm{m^3\,s^{-1}}$. **b**, Aerial photograph showing the location of the abandoned channel boulder bar (outlined in white). Aerial imagery courtesy of the US Department of Agriculture. **c**, Field photo of the boulder deposit shown in **b**; the median grain size of clasts on the bar is 0.15 m. The photo is taken near the tip of the arrow in **b** and the view is downstream; person (circled) for scale.
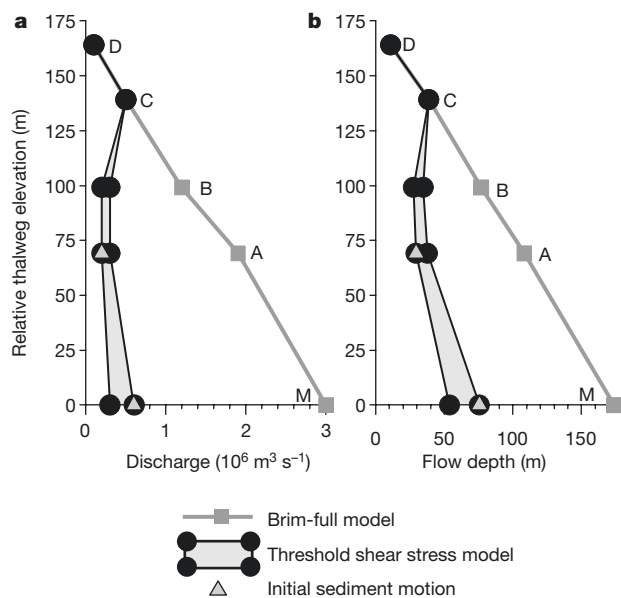
Figure 3 | Simulated discharge and water depths. a, b, Discharge (**a**) and water depths (**b**) predicted by the brim-full model, by the threshold shear stress model, and from criteria related to the initial motion of sediment. The shading shows the range of predicted values based on upper- and lower-bound parameterizations of the critical dimensionless shear stress for bedrock incision by block sliding (see Methods). The letters A–D indicate simulation results for bed elevations A–D; M denotes results for the modern topography. Relative thalweg elevations denote the elevation of the palaeo-channel floor above the modern channel floor.

formation is of similar order to previous estimates for other Channeled Scablands canyons[11]. By contrast, the discharges predicted by the threshold shear stress model are lower by approximately an order of magnitude, with incision from the upper-most terrace to the canyon floor achieved by discharges of at most $0.6 \times 10^6\,\mathrm{m}^3\,\mathrm{s}^{-1}$ (Fig. 3a), and the predicted discharges change only slightly during canyon formation. Water depths predicted by the threshold shear stress model are 27–76 m, whereas the brim-full hypothesis predicts increasing water depths during canyon formation with a peak at 175 m (Fig. 3b). The narrow range of discharge rates predicted by the threshold shear stress model is consistent with the incision occurring during a single flood[5] or during multiple floods of similar magnitude[9], as would be expected for floods issuing repeatedly from the same ice-dammed lake[24].

The Great Gravel Bar in upper Moses Coulee is inundated at a modelled discharge of $0.6 \times 10^6\,\mathrm{m}^3\,\mathrm{s}^{-1}$ (Fig. 2a), which is consistent with the upper discharge estimate predicted by the threshold shear stress model and with observations that indicate that bars tend to aggrade to near the height of the flood[27]. The bar at the abandoned channel site is made up of well-rounded basalt clasts with a median diameter of 0.15 m, indicating that they were transported as bedload. Bar deposition by bedload is consistent both with discharges predicted by the threshold shear stress model (because modelled bed shear stresses at the bar just exceed the threshold of motion) and with the formation regime of bars in rivers with coarse-grained bed sediment[28]. Shear stresses predicted by the brim-full model would have exceeded the threshold of suspension for the majority of the boulders on the bar (which have diameters of less than 0.5 m), which is inconsistent with the field evidence for bedload deposition. The morphology and sedimentology of the depositional bars are therefore more consistent with the threshold shear stress end-member than with the brim-full end-member.

Bed stresses on some parts of the knickzone in the central part of Moses Coulee are several-fold higher than the thresholds for plucking, for discharges that are consistent with the threshold shear stress model (Fig. 1b, d). If flood waters no longer reached the height of the terraces because they were abandoned by lowering of the channel bed as the
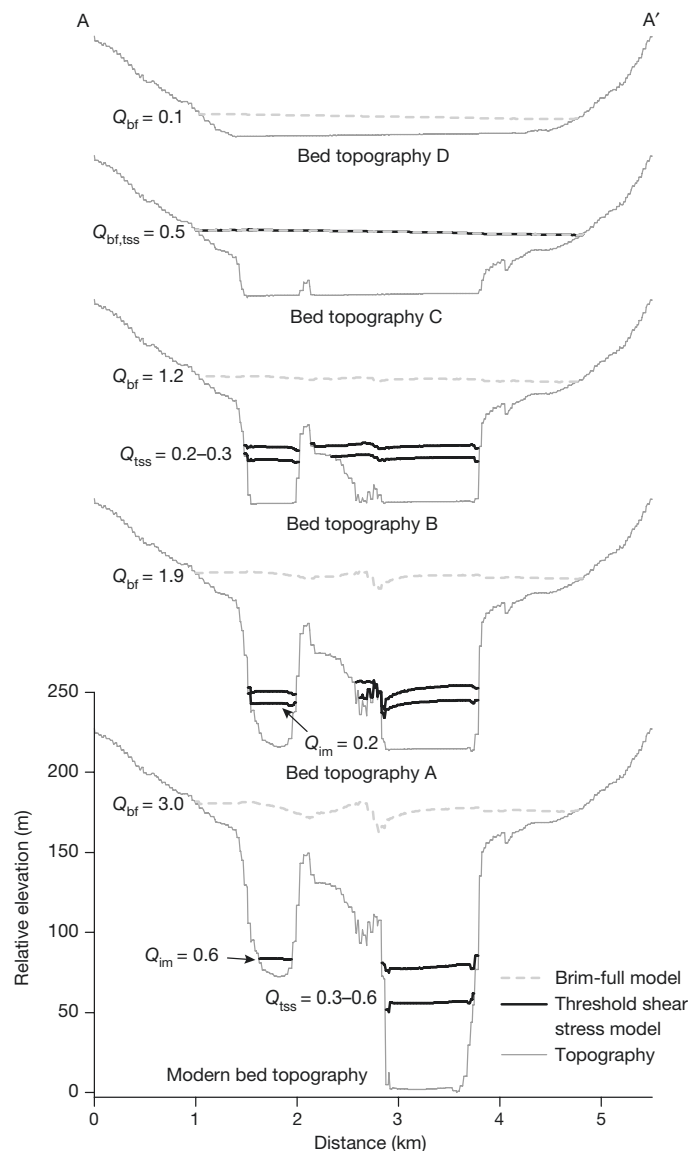
Figure 4 | Co-evolution of topography and flood level predicted by the brim-full and threshold shear stress models. Q_{bf}, Q_{tss} and Q_{im} refer to discharges predicted by brim-full, threshold shear stress and sediment initial motion criteria, respectively, with units of $10^6\,\mathrm{m}^3\,\mathrm{s}^{-1}$. The location of the cross-section (A–A') is shown in Fig. 1d.

knickzone retreated upstream, as is probably the case, then the higher shear stresses on the steep channel bed[29] indicate that the knickzone was probably a site of transient, rapid erosion, provided that the well-jointed Columbia River basalts are indeed mechanically similar to cohesionless or weakly interlocked bedrock blocks.

The threshold shear stress model implies that canyons in the Channeled Scablands were eroded by floods with depths that were a fraction of the relief of the final canyon (Fig. 4). This physics-based finding is consistent with several recent investigations of canyon carving at other sites on Earth and Mars: for example, those where bedrock incision by plucking or toppling of jointed rock occurs at depths less than brim-full[5,16–18,23], those where terrace chronology indicates multiple episodes of canyon incision[9,20], or those where lakes in breached craters contain insufficient water volumes to fill downstream channels[19].

Our results suggest that the morphology of canyons (for example, terraces, valley shapes and slope profiles) on Earth and Mars could reveal information about both the history and discharge of flooding that warrants further investigation. The outburst floods that carved the

Channeled Scablands were extraordinary under either end-member model, but predictions of discharges from the threshold shear stress model are five- to ten-fold smaller. On Mars, owing to the low permeability of aquifers, it has been challenging to reconcile the very large reconstructed brim-full discharges in outflow channels with a subsurface flood source[30]. Given the proposed similarity in incision mechanics for outflow channels on Mars and in the Channeled Scablands[2,16,20,22,23], the threshold shear stress model provides a link between the physics of groundwater-sourced floods and terraces observed in orbital data[20], implying longer duration, lower discharge floods, or multiple floods on early Mars[30].

Online Content Methods, along with any additional Extended Data display items and Source Data, are available in the online version of the paper; references unique to these sections appear only in the online paper.

1. Bretz, J. H. The Channeled Scablands of the Columbia Plateau. *J. Geol.* **31,** 617–649 (1923).
2. Baker, V. R. *The Channels of Mars* (Univ. Texas Press, 1982).
3. Carr, M. H. Mars: a water-rich planet? *Icarus* **68,** 187–216 (1986).
4. Barber, D. *et al.* Forcing of the cold event of 8,200 years ago by catastrophic drainage of Laurentide lakes. *Nature* **400,** 344–348 (1999).
5. Lamb, M. P. & Fonstad, M. A. Rapid formation of a modern bedrock canyon by a single flood event. *Nat. Geosci.* **3,** 477–481 (2010).
6. Bretz, J. H. The Lake Missoula floods and the Channeled Scabland. *J. Geol.* **77,** 505–543 (1969).
7. O'Connor, J. E., Grant, G. E. & Costa, J. E. in *Ancient Floods, Modern Hazards: Principles and Applications of Paleoflood Hydrology* (eds House, P. K. *et al.*) 359–385 (American Geophysical Union, 2002).
8. Baker, V. *et al.* Ancient oceans, ice sheets and the hydrological cycle on Mars. *Nature* **352,** 589–594 (1991).
9. Baynes, E. R. *et al.* Erosion during extreme flood events dominates Holocene canyon evolution in northeast Iceland. *Proc. Natl Acad. Sci. USA* **112,** 2355–2360 (2015).
10. Carr, M. H. Formation of Martian flood features by release of water from confined aquifers. *J. Geophys. Res. Solid Earth* **84,** 2995–3007 (1979).
11. Baker, V. R. *Paleohydrology and Sedimentology of Lake Missoula Flooding in Eastern Washington.* GSA Special Paper 144 (Geological Society of America, 1973).
12. Denlinger, R. & O'Connell, D. Simulations of cataclysmic outburst floods from Pleistocene Glacial Lake Missoula. *Geol. Soc. Am. Bull.* **122,** 678–689 (2010).
13. O'Connor, J. E. & Baker, V. R. Magnitudes and implications of peak discharges from glacial Lake Missoula. *Geol. Soc. Am. Bull.* **104,** 267–279 (1992).
14. Komar, P. D. Comparisons of the hydraulics of water flows in Martian outflow channels with flows of similar scale on Earth. *Icarus* **37,** 156–181 (1979).
15. Miyamoto, H. *et al.* Cataclysmic Scabland flooding: insights from a simple depth-averaged numerical model. *Environ. Model. Softw.* **22,** 1400–1408 (2007).
16. Lamb, M. P., Mackey, B. H. & Farley, K. A. Amphitheater-headed canyons formed by megaflooding at Malad Gorge, Idaho. *Proc. Natl Acad. Sci. USA* **111,** 57–62 (2014).
17. Lamb, M. P., Dietrich, W. E., Aciego, S. M., DePaolo, D. J. & Manga, M. Formation of Box Canyon, Idaho, by megaflood: implications for seepage erosion on Earth and Mars. *Science* **320,** 1067–1070 (2008).
18. Anton, L., Mather, A., Stokes, M., Muñoz-Martin, A. & De Vicente, G. Exceptional river gorge formation from unexceptional floods. *Nat. Commun.* **6,** 7963 (2015).
19. Coleman, N. M. Hydrographs of a Martian flood from a breached crater lake, with insights about flow calculations, channel erosion rates, and chasma growth. *J. Geophys. Res. Planets* **118,** 263–277 (2013).
20. Warner, N., Gupta, S., Muller, J., Kim, J. & Lin, S. A refined chronology of catastrophic outflow events in Ares Vallis, Mars. *Earth Planet. Sci. Lett.* **288,** 58–69 (2009).
21. Lamb, M. P., Finnegan, N. J., Scheingross, J. S. & Sklar, L. S. New insights into the mechanics of fluvial bedrock erosion through flume experiments and theory. *Geomorphology* **244,** 33–55 (2015).
22. Lamb, M. P. & Dietrich, W. E. The persistence of waterfalls in fractured rock. *Geol. Soc. Am. Bull.* **121,** 1123–1134 (2009).
23. Lapotre, M. G. A., Lamb, M. P. & Williams, R. M. E. Canyon formation constraints on the discharge of catastrophic outburst floods of Earth and Mars. *J. Geophys. Res. Planets* **121,** 1232–1263 (2016).
24. Waitt, R. B. Case for periodic, colossal jökulhlaups from Pleistocene glacial Lake Missoula. *Geol. Soc. Am. Bull.* **96,** 1271–1286 (1985).
25. Parker, G. Self-formed straight rivers with equilibrium banks and mobile bed. Part 2. The gravel river. *J. Fluid Mech.* **89,** 127–146 (1978).
26. Wohl, E. E. Bedrock benches and boulder bars: floods in the Burdekin Gorge of Australia. *Geol. Soc. Am. Bull.* **104,** 770–778 (1992).
27. Schmidt, J. C., Grams, P. E. & Leschin, M. F. in *The Controlled Flood in Grand Canyon* (eds Webb, R. H. *et al.*) 185–203 (American Geophysical Union, 1999).
28. Church, M. Bed material transport and the morphology of alluvial river channels. *Annu. Rev. Earth Planet. Sci.* **34,** 325–354 (2006).
29. Venditti, J. G. *et al.* Flow in bedrock canyons. *Nature* **513,** 534–537 (2014).
30. Andrews-Hanna, J. C. & Phillips, R. J. Hydrological modeling of outflow channels and chaos regions on Mars. *J. Geophys. Res. Planets* **112,** E08001 (2007).

Author Contributions I.J.L. and M.P.L. designed the study and wrote the manuscript. I.J.L. conducted the hydraulic simulations.

Author Information Reprints and permissions information is available at www.nature.com/reprints. The authors declare no competing financial interests. Readers are welcome to comment on the online version of the paper. Correspondence and requests for materials should be addressed to I.J.L. (ilarsen@umass.edu).

Reviewer Information *Nature* thanks J. Venditti and the other anonymous reviewer(s) for their contribution to the peer review of this work.

METHODS

Hydraulic modelling. Outburst floods through Moses Coulee were simulated using ANUGA version 2.0, a finite-volume hydrodynamic model that conserves mass and momentum by solving the two-dimensional, time-dependent, depth-averaged, shallow-water equations on a triangular mesh[31,32]. The size of the triangular mesh was varied spatially, with a maximum triangle area of 900 m[2] for the main study reach and 5,000 m[2] elsewhere (Extended Data Fig. 1).

Floods were simulated with five different topographic boundary conditions: the modern topography and four topographies with reconstructed bed elevations (A–D). We simulated the hydraulic conditions through inferred stages of canyon evolution that we reconstructed from terraces. The reconstructed bed elevations were based on the elevations of bedrock terraces found downstream of a prominent knickzone and maintain the same bed slope as the channel upstream from the knickzone (Fig. 1; Extended Data Fig. 2). Although we do not explicitly simulate lateral knickpoint retreat, which probably accounted for much of the erosion of Moses Coulee, the decrease in bed elevation that we impose for different simulations mimics the vertical bed lowering that would have occurred as knickpoints migrated upstream, past the reach with preserved terraces. If slopes were steeper than the modern topography during canyon incision and erosion was limited to steep reaches[29], then the discharges predicted by our threshold shear stress model are upper estimates; the hydraulic simulations indicate that even the smallest floods we simulated produce shear stresses across the knickzone that exceed the threshold for block sliding (Extended Data Fig. 3).

The topographic data were from 10-m digital elevation model (DEM) data derived from US Geological Survey (USGS) topographic maps. DEM and reconstructed topographic data were used by ANUGA to generate the triangular mesh.

ANUGA implements bed friction with Manning's roughness coefficient (n). We determine the roughness coefficient by equating a form of the Manning–Strickler relation[33]

$$\frac{u}{u_*} = 8.1\left(\frac{h}{k_s}\right)^{1/6}$$

and the Manning equation

$$u = \frac{h^{2/3}S^{1/2}}{n}$$

and re-arranging for n:

$$n = \frac{1}{8.1}\frac{k_s^{1/6}}{g^{1/2}}$$

Here u is flow velocity, $u_* = \sqrt{C_f}u$ is bed shear velocity, C_f is a friction coefficient, g is acceleration due to gravity, h is flow depth, S is the tangent of the channel-bed angle and k_s is a bed-roughness length scale. We assume that k_s follows a relation proposed for bedrock channels:

$$k_s = r_d r_{br} \sigma_{br}$$

where r_d and r_{br} are hydraulic roughness scaling parameters and σ_{br} is one standard deviation of the elevation of the bedrock bed[34]. We set $r_d = 2$ and assume $r_{br} = 2$, which is within the range of reported values[34]. The mean of σ_{br} from five different reaches in our study area was about 5 m; consequently, we determined that $n = 0.065$ and assume that this roughness coefficient is spatially uniform. The USGS 10-m DEM was used to determine roughness.

For each flood simulation, a constant discharge was input at the upstream boundary of the model domain and flow evolved within the domain before exiting at the downstream boundary[32]. The duration of each simulation was 10,000 s, which was sufficient for the flow to evolve to near steady-state (Extended Data Fig. 4). Model outputs for flood elevation (stage) and the x and y components of momentum and velocity were saved every 100 s and gridded to a pixel resolution of 30 m × 30 m, a value selected because it is comparable to the maximum triangle area in the study reach. The 10 grids from the final 1,000 s of each simulation were averaged. From the averaged grids, flow depth (h) was calculated as the difference in mean flood stage and bed topography, streamwise velocity (u) was determined by the vector sum of the x and y velocity components, and bed shear stress (τ_b) was calculated as $\tau_b = \rho C_f u^2$, where ρ is the density of water. The friction coefficient is related to Manning's n by

$$C_f = \frac{gn^2}{h^{1/3}}$$

Discharge predicted by the brim-full model. The discharge predicted by the brim-full model was determined by iteratively simulating floods in discharge increments of 0.1×10^6 m^3 s^{-1} through the modern topography and identifying the discharge scenario in which the simulated flood stage reached the brim-full level determined from field evidence. Field evidence for the elevation of the brim-full level was a scarp cut into loess with rounded basalt clasts deposited at its base.

Discharge predicted by the threshold shear stress model. Theoretical and field evidence from gravel-bedded rivers demonstrates that bed shear stresses can exceed the threshold for sediment transport by a factor of only about 1.2 on average before the channel cross-section erodes and evolves to a form that maintains shear stresses near the threshold for sediment transport[25]. Ultimately, to form a stable alluvial channel, the channel banks must be below the threshold for erosion, whereas the bed must be above the threshold for transport. If the bed and banks are composed of the same material, which is the case both for gravel-bed rivers and the Channeled Scablands, then the channel-forming shear stress for self-formed channels cannot greatly exceed the conditions required for sediment entrainment. The similarity in low excess shear stress (factor of 1.1–1.6) required to erode gravel-bedded channels and the channel at Canyon Lake Gorge, Texas[5], suggests that the mechanics of erosion and sediment transport in gravel-bedded rivers are similar to those in bedrock channels formed in well-jointed bedrock, where plucking of bedrock blocks is the dominant erosion mechanism[6,11,21], leading to the threshold shear stress end-member model for canyon formation. A similar threshold stress mechanism has also been proposed at waterfalls dominated by toppling, which are common to Scabland terrain[23].

The threshold shear stress model predicts that channel bed stresses should be at or near the threshold for plucking, but local deviations are observed (Fig. 1) and expected for a variety of reasons, consistent with observations in threshold alluvial rivers. Anomalies are likely to occur where areas of the bed are eroding faster, such as in knickzones, in areas where heterogeneity in rock strength both within and among basalt flows leads to differing fracture spacing and block size (leading to, for example, differences in canyon width), and in areas where the formation of backwaters locally lowers bed stresses. For example, our simulations assume a constant block size of 0.5 m; accounting for a wider range of block sizes would produce an equally wider range of expected threshold stresses for plucking (equation (1)). The threshold shear stress model predicts that, over time, the topography is likely to evolve such that bed protrusions are eroded and knickpoints are transient and retreat, such that shear stresses, on average, tend towards the threshold values for erosion. For Moses Coulee, 67% of the terrain has simulated bed stresses within the bounds for plucking blocks of the size found in depositional bars in the Channeled Scablands (0.13–0.83 m), which is consistent with the threshold shear stress model; for brim-full flow, only 33% of the terrain has simulated bed stresses within the plucking bounds for the same range of block sizes (Extended Data Fig. 5).

Plucking—the removal of bedrock blocks—is the dominant erosion mechanism in the well-jointed basalt bedrock of the Channeled Scablands[6,22]. Experimental studies have shown that downstream sliding of blocks can be the dominant form of plucking[35]. Therefore, to evaluate the discharges predicted by the threshold shear stress model, we first determined the dimensionless critical shear stress for block sliding:

$$\tau_{pc}^* = \frac{\cos(\theta)[\tan(\phi) - \tan(\theta)] + 2\tau_w^*}{\left[1 + \frac{1}{2}C_D\left(\frac{u}{u_*}\right)^2\frac{P}{L}\right][1 + F_L^*\tan(\phi)]}$$

where θ is the bed angle, ϕ is the bed friction angle, τ_w^* is the dimensionless block sidewall stress, C_D is the local drag coefficient, P is the block protrusion height (or equivalently the roughness on the top of the block), L is the block length and F_L^* is the dimensionless hydraulic lift force[21]. We set $\theta = 1°$ on the basis of measurements of the topographic slope outside of the channel upstream from the terraces in Moses Coulee. The friction angle was assumed to be 34°, consistent with the range of values (31°–36°) for wet basalt[36]. The ratio of block protrusion height to block length (P/L) was set to 0.2 on the basis of field observations. The quantities C_D, u/u_* and F_L^* were taken to be 1, 8.3 and 0.85, respectively[21]. Dimensionless block sidewall stress is poorly constrained, so we varied the values between 0 and 0.2 to predict a range of potential values for τ_{pc}^*. The Columbia River basalts are jointed and fractured, commonly exhibiting colonnade and entablature structures[37]. The fractures reduce the cohesive strength of the Columbia River basalts by one or two orders of magnitude relative to intact basalt[38]. A dimensionless block sidewall stress of 0 is appropriate for the wide, open joints we observed between basalt columns while in the field, and 0.2 corresponds to interlocking or cohesion between blocks with a wall stress that is 20% of the block weight per unit area. Greater assumed cohesive strength or interlocking would lead to higher discharge estimates for the threshold shear stress model. The range of τ_{pc}^* was then used to calculate upper and lower bounds on the critical shear stress for block sliding:

$$\tau_{pc} = \tau_{pc}^*(\rho_s - \rho)gD \tag{1}$$

where ρ_s is the density of the basalt ($2{,}800\,\mathrm{kg\,m^{-3}}$) and D is the block height[21]. We set $D = 0.5\,\mathrm{m}$, a value consistent with the dimensions of basalt columns[39] in the Channeled Scablands and that falls within the range of median intermediate-axis diameters (D_{50}) of boulders we measured on the Ephrata Fan ($D_{50} = 0.30\,\mathrm{m}$, sample size $N = 138$) and in Drumheller Channels ($D_{50} = 0.59\,\mathrm{m}$, $N = 301$) (Extended Data Fig. 6). The Ephrata Fan and Drumheler Channels sites are located in a different floodway approximately 30 km and 70 km to the southeast of Moses Coulee, respectively[6]. The lower and upper shear stress bounds for erosion by sliding calculated by this method (based on varying the end-member block sidewall stress values from 0 to 0.2) are 467 Pa and 751 Pa, respectively.

Unlike the brim-full discharge model, which predicts discharge for the length of an entire channel reach, the threshold shear stress model makes predictions for local bed shear stress within the channel. We therefore determined the mean and standard deviation of shear stress at 12 locations placed approximately along a cross-section within the study reach, which span an elevation range from the channel floor to the highest terrace (Extended Data Fig. 7). To determine the discharges predicted by the threshold shear stress model, we used the upper and lower shear stress bounds for plucking by sliding shown in Extended Data Fig. 8 to define the widest possible bounds on flood discharge that satisfy the model conditions for all eroding sites.

For a given topographic reconstruction, corresponding to the modern topography or to one of our four inferred stages of canyon incision, we first used the upper and lower thresholds for plucking to define the range of possible discharges at the lowest elevation site that are consistent with the threshold shear stress model. For the modern topography, for example, the lowest site corresponds to the modern canyon floor (Extended Data Fig. 7). We then found the discharge range, following the same procedure, at sites with progressively higher elevations that produced bed stresses that were within the bounds for plucking at the site of interest and also for all lower elevation sites (Extended Data Fig. 9). These two criteria are important because, for a flood discharge to be consistent with the threshold stress model, all inundated and eroding sites from the canyon floor upward must have bed stresses that are within the bounds for plucking. Most brim-full discharge scenarios violate these constraints because they produce bed stresses on the canyon floor that greatly exceed the bounds on plucking (Extended Data Fig. 8). For the threshold shear stress model, if the discharge required to pluck blocks at a higher elevation site exceeds that of a lower elevation site, then the higher sites were considered to be dry and abandoned and therefore were not used to define the range of discharges for that stage of canyon incision (Extended Data Fig. 9). This analysis therefore allows for identification, for a given topographic reconstruction, of the maximum range in flood discharges that is consistent with the threshold shear stress model, for both the canyon floor and all higher elevation surfaces that could have been inundated. The procedure was repeated for the modern topography and the topographies for each of the four stages of canyon incision to define discharges, flow depths, cross-sectional areas and channel widths (Fig. 3, Extended Data Fig. 10).

Thresholds for sediment transport and suspension. The abandoned channel on the south side of the study reach contains a gravel-boulder bar with well-rounded clasts (Fig. 2b, c). We measured the intermediate diameter of 220 individual clasts measured at 1-m spacing along a grid (excluding loess deposited after flooding) and calculated $D_{50} = 0.15\,\mathrm{m}$ and $D_{84} = 0.41\,\mathrm{m}$ (84th percentile of clast diameters are finer than this size) (Extended Data Fig. 6). We calculated the critical shear stress for initial sediment motion (τ_b) by substituting $\tau_c^* = 0.045$ for τ_{pc}^* and D_{50} for D in equation (1). The resulting critical shear stress for initial motion is 119 Pa. The threshold for sediment suspension was calculated as[40] $\tau_b = \rho(0.4w_s)^2$, where w_s, the terminal settling velocity, is defined as

$$w_s = \frac{RgD^2}{C_1\nu + [0.75C_2RgD^3]^{0.5}}$$

in which R is submerged specific gravity (1.8 for basalt in water), $C_1 = 20$ and $C_2 = 1.1$ are constants representing natural sediment, and ν is the kinematic viscosity of water[41]. The shear stress threshold for suspension of D_{50} is 513 Pa and for $D = 0.5\,\mathrm{m}$ is 1,712 Pa, which is similar to the modelled brim-full shear stress at the bar for the modern topography (1,706 Pa), but inconsistent with bar deposition by bedload transport.

Code availability. The hydrodynamic code ANUGA is open-source and available for download at https://anuga.anu.edu.au/. The PYTHON scripts used to implement ANUGA are available from the authors by request.

Data availability. Digital elevation data are available from the University of Washington Geomorphological Research Group website (http://gis.ess.washington.edu/data/). All simulation results and data are available from the authors by request.

31. Roberts, S. G., Nielsen, O. M. & Jakeman, J. in *Modeling, Simulation and Optimization of Complex Processes* (eds Bock, H.G. *et al.*) 489–498 (Springer, 2008).
32. Roberts, S., Nielsen, O., Gray, D., Sexton, J. & Davies, G. *ANUGA User Manual. Release 2.0.* https://github.com/GeoscienceAustralia/anuga_core/raw/master/doc/anuga_user_manual.pdf (2015).
33. Parker, G. Selective sorting and abrasion of river gravel. II: applications. *J. Hydraul. Eng.* **117**, 150–171 (1991).
34. Johnson, J. P. A surface roughness model for predicting alluvial cover and bed load transport rate in bedrock channels. *J. Geophys. Res. Earth Surface* **119**, 2147–2173 (2014).
35. Dubinski, I. M. & Wohl, E. Relationships between block quarrying, bed shear stress, and stream power: a physical model of block quarrying of a jointed bedrock channel. *Geomorphology* **180–181**, 66–81 (2013).
36. Selby, M. J. *Hillslope Materials and Processes* 93 (Oxford Univ. Press, 1993).
37. Long, P. E. & Wood, B. J. Structures, textures, and cooling histories of Columbia River basalt flows. *Geol. Soc. Am. Bull.* **97**, 1144–1155 (1986).
38. Schultz, R. Limits on strength and deformation properties of jointed basaltic rock masses. *Rock Mech. Rock Eng.* **28**, 1–15 (1995).
39. Ehlmann, B. L., Viles, H. A. & Bourke, M. C. Quantitative morphologic analysis of boulder shape and surface texture to infer environmental history: a case study of rock breakdown at the Ephrata Fan, Channeled Scabland, Washington. *J. Geophys. Res. Earth Surface* **113**, F02012 (2008).
40. NiÑo, Y., Lopez, F. & Garcia, M. Threshold for particle entrainment into suspension. *Sedimentology* **50**, 247–263 (2003).
41. Ferguson, R. & Church, M. A simple universal equation for grain settling velocity. *J. Sediment. Res.* **74**, 933–937 (2004).
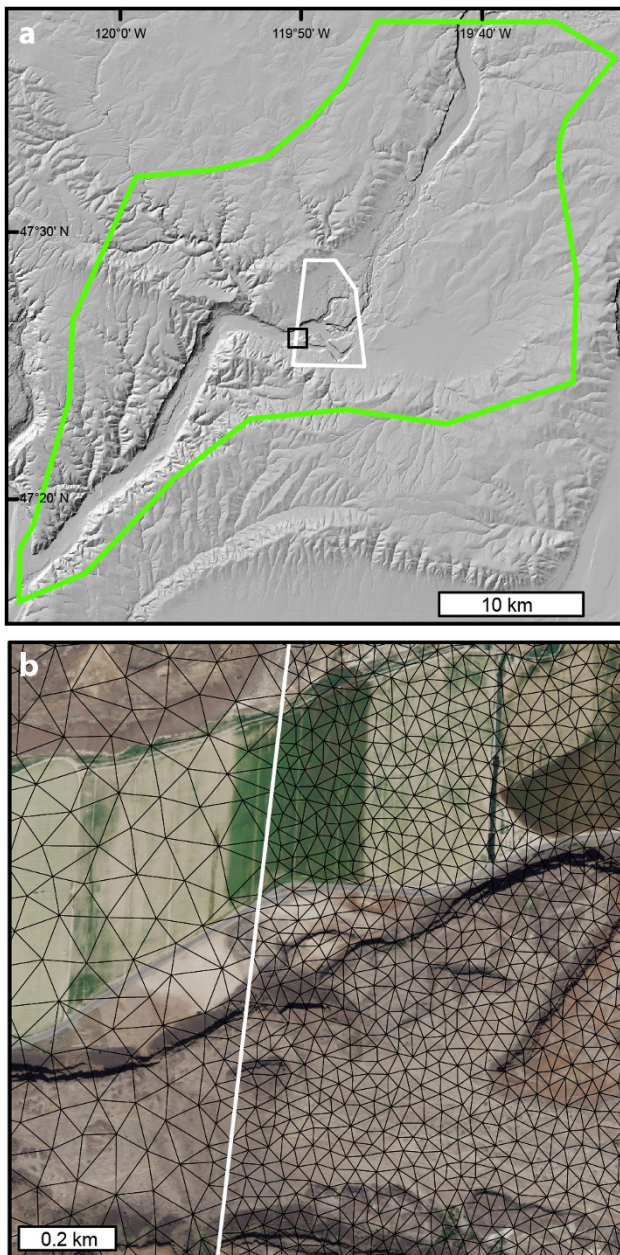
Extended Data Figure 1 | Computational mesh resolution. a, Map of the computational domain (green outline). Black square shows the location of **b**. **b**, Map showing the different triangular mesh resolutions within the computational domain, with a maximum triangle area of 900 m^2 within the white polygon in **a** and 5,000 m^2 throughout the rest of the domain. We used a smaller triangle area in the study reach (within the white polygon) to better resolve spatial variability in shear stresses and a slightly larger triangle area elsewhere for computational efficiency.
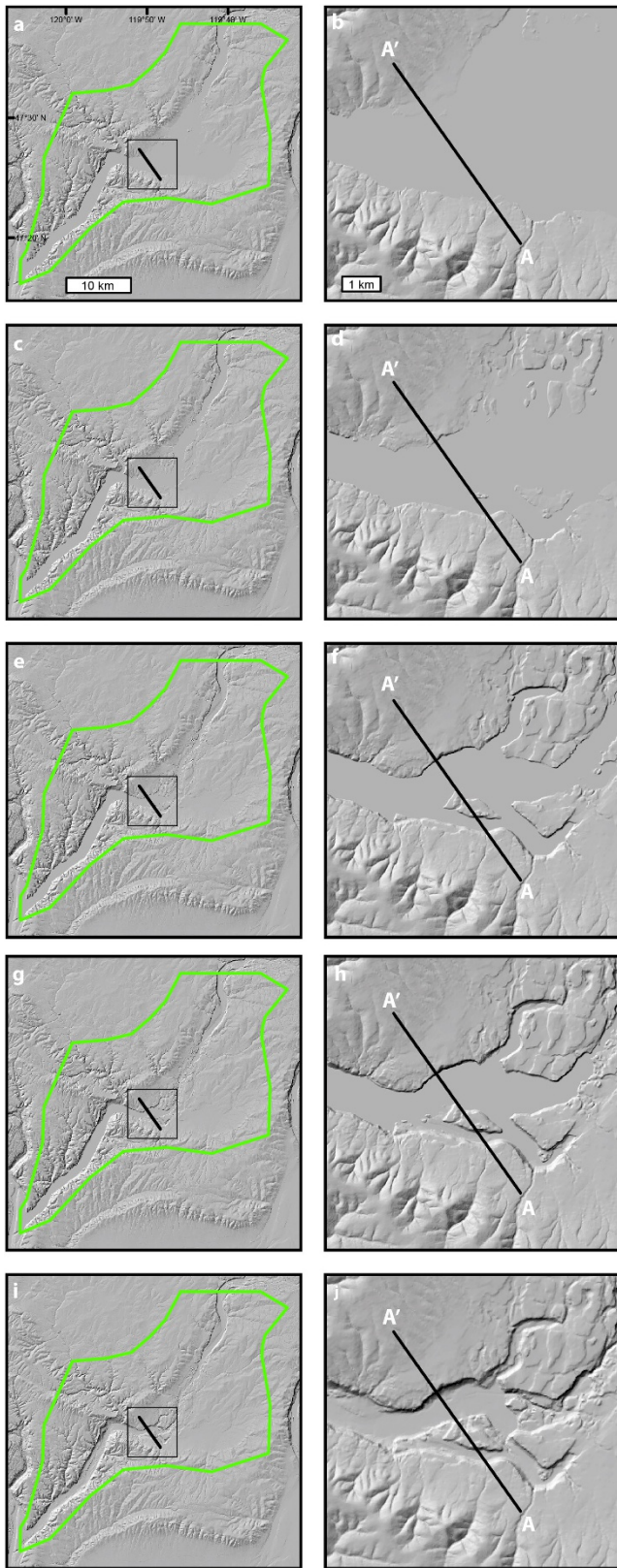
Extended Data Figure 2 | Hillshade maps of the study reach for each bed elevation. These maps depict the reconstructed topography in Moses Coulee, which is based on the elevation of terraces and the modern channel bed upstream from the knickzone. **a**, **b**, Bed elevation D; **c**, **d**, bed elevation C; **e**, **f**, bed elevation B; **g**, **h**, bed elevation A; **i**, **j**, modern topography.
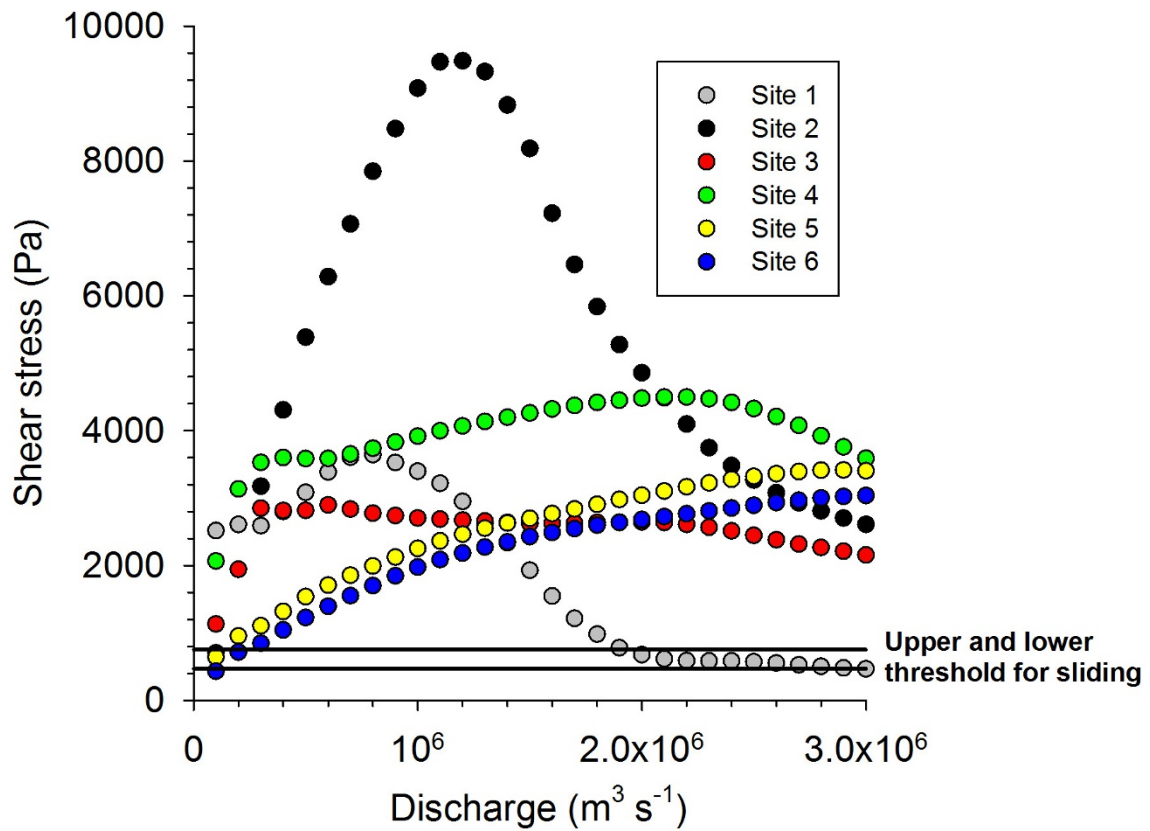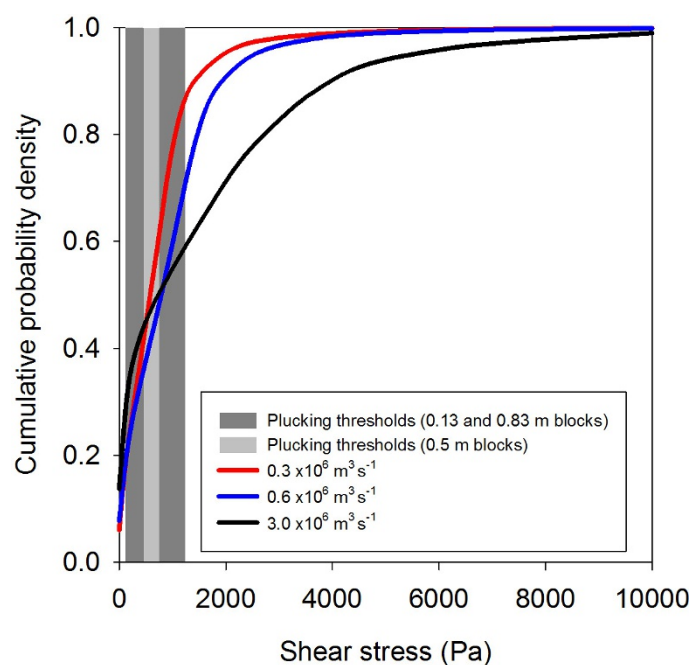
Extended Data Figure 3 | Bed shear stress as a function of discharge for sites on the Moses Coulee knickzone. Data correspond to locations shown in Extended Data Fig. 7. For nearly all simulated discharges, the modelled shear stresses on the knickzone exceed the thresholds for plucking via block sliding, indicating that the knickzone would probably have been rapidly eroding during floods or that it is made up of stronger rock.
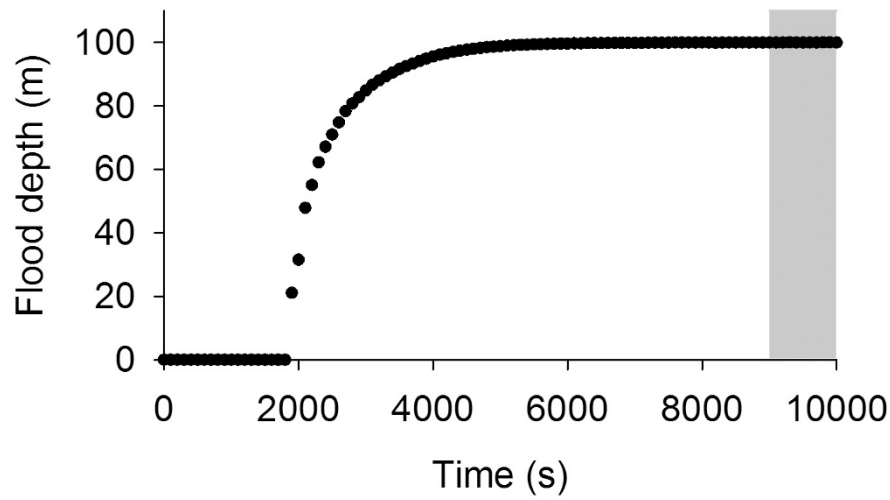
Extended Data Figure 4 | Flood depth versus time for a typical simulation. The example shown is a flood with a discharge of $10^6\, m^3\, s^{-1}$ routed through the modern topography. The grey box shows the final ten time-steps, from which the model results (stage, velocity, shear stress and so on) were extracted and used to produce time-averaged grids to reduce the influence of transient waves relative to data from a single time-step.

Extended Data Figure 5 | Cumulative bed stress probability density functions. The light grey bar shows the lower (467 Pa) and upper (751 Pa) threshold shear stress bounds for plucking of 0.5-m blocks. The dark grey bar shows the threshold stress bounds (117 Pa and 1,242 Pa) assuming a wider distribution of block sizes of 0.13–0.83 m, based on the D_{16} and D_{84} (16th and 84th percentiles) of basalt clasts at the Ephrata Fan and Drumheller Channels sites, respectively (Extended Data Fig. 6). Cumulative probability density functions are shown for the brim-full flood (discharge of 3.0×10^6 m^3 s^{-1}; black line) and the lower (0.3×10^6 m^3 s^{-1}; red line) and upper (0.6×10^6 m^3 s^{-1}; blue line) flood discharge bounds predicted by the threshold shear stress model for the modern Moses Coulee topography. Data are extracted from each grid cell within the entire length of Moses Coulee (Fig. 1b). For the brim-full flood, only 8% of the terrain of Moses Coulee has modelled bed shear stresses within the bounds for plucking 0.5-m blocks, and this increases to 33% when considering the wider range of block sizes; some areas have extremely high bed stresses of more than 10,000 Pa. In contrast, for discharges predicted by the threshold shear stress model, 25% of the terrain has shear stresses within the bounds for plucking 0.5-m blocks, and this increases to 67% when considering a wider distribution of block sizes. This high proportion of bed stresses within the plucking threshold range, relative to the brim-full flood, is consistent with the hypothesis that the channel adjusts so that a large portion of the terrain is near the threshold state during megaflood incision. Note that the study locations in Extended Data Fig. 7 were used to define the discharge bounds for the threshold shear stress model, so all of those locations have bed stresses within the plucking threshold range by definition (see Extended Data Fig. 8).
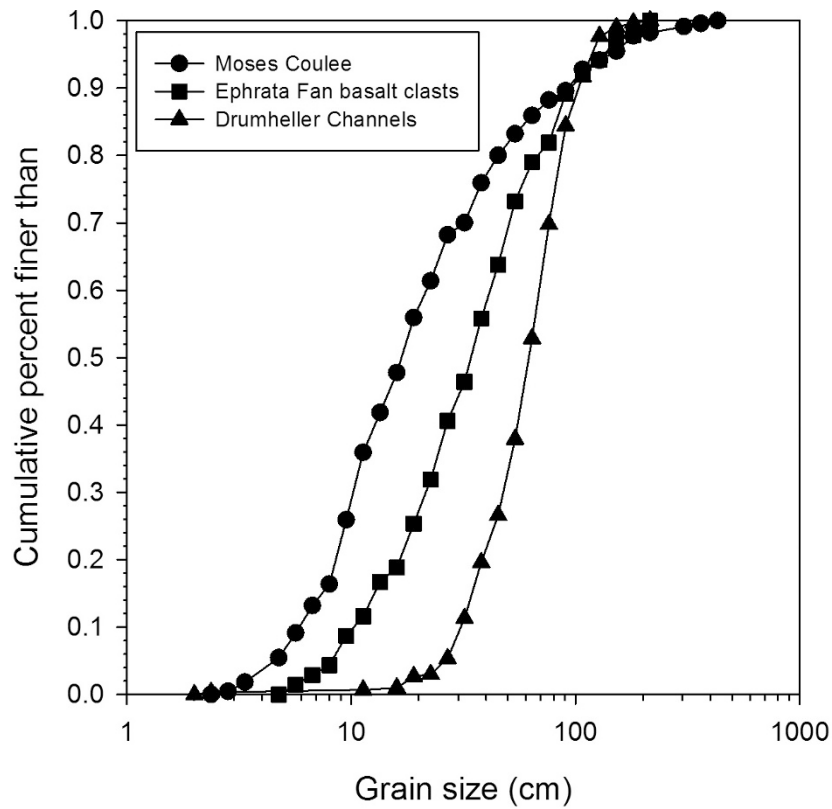
Extended Data Figure 6 | Boulder size data. Cumulative grain-size distribution for the Moses Coulee abandoned channel boulder bar (circles), Ephrata Fan basalt clasts (squares) and the Drumheller Channels boulder bar (triangles). Measurements were made of the intermediate grain diameter using a Wolman-style pebble count. The Ephrata Fan and Drumheller Channels sites are to the southwest of Moses Coulee and in a different flood pathway. The larger boulders at the Ephrata Fan and Drumheller Channels are assumed to originate as basalt columns that have been rounded by fluvial transport.
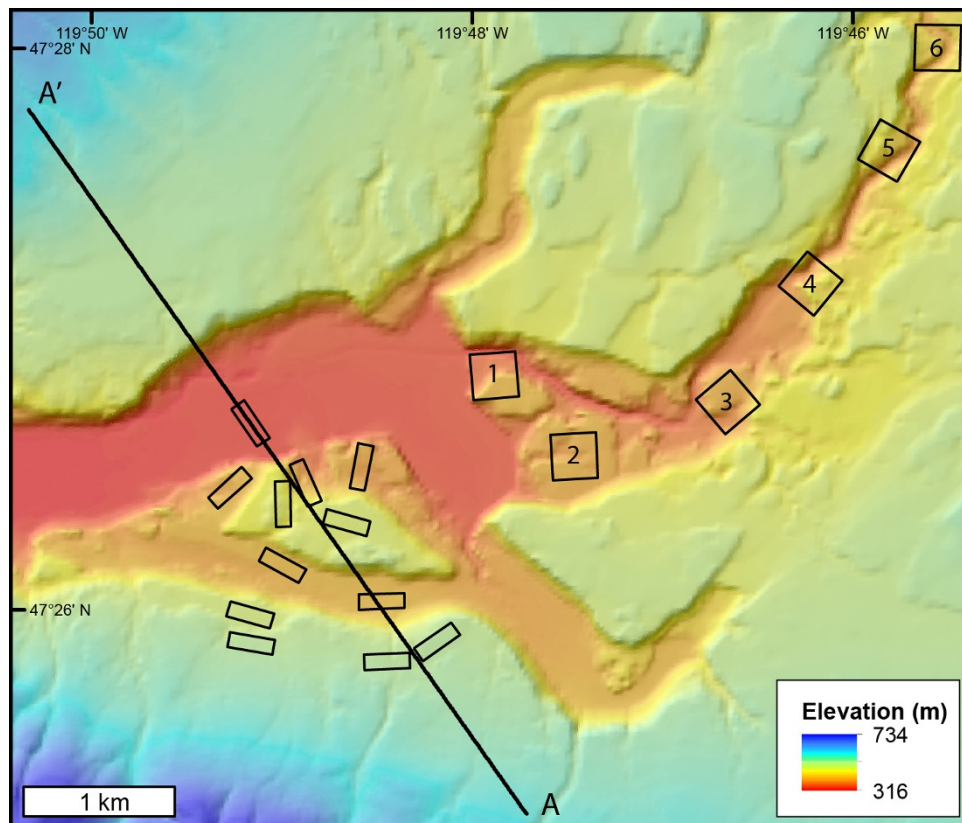
Extended Data Figure 7 | Locations of the areas used to calculate mean bed shear stress. The 30,000-m^2 rectangles near the A–A′ cross-section were used to constrain discharges predicted by the threshold shear stress model. The larger 90,000-m^2 polygons (labelled 1–6) were used to determine the shear stresses on the knickzone; the numbers correspond to the data in Extended Data Fig. 3.
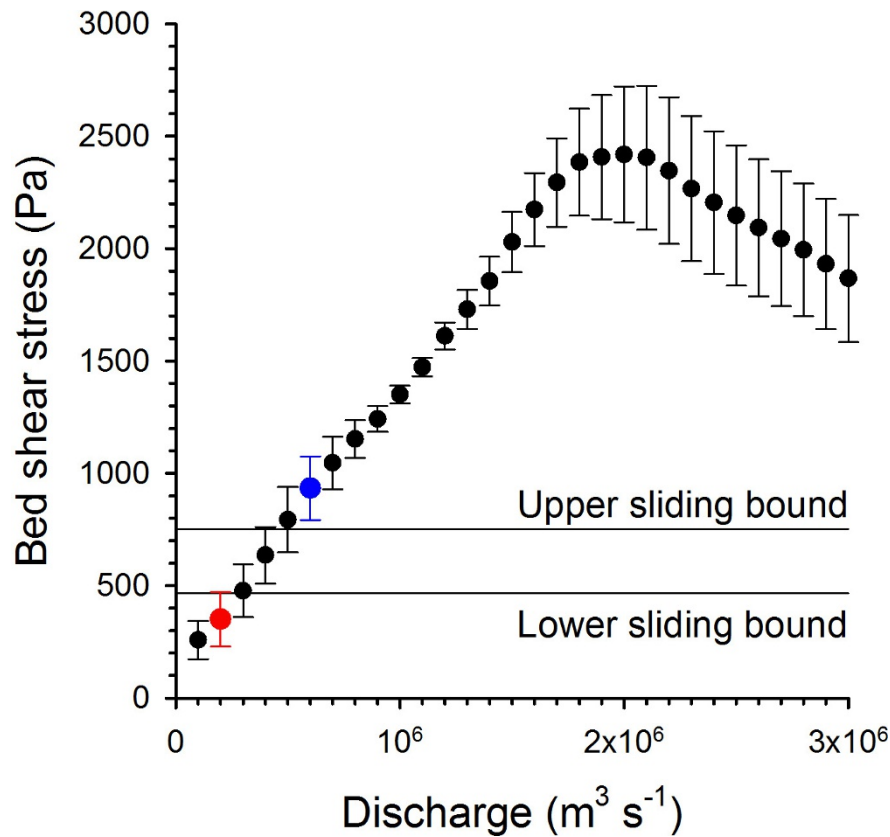
Extended Data Figure 8 | Example model output showing the upper and lower shear stress thresholds for block sliding. Round symbols depict the mean and bars depict one standard deviation ($n = 33$) of bed shear stress values extracted from one of the twelve 30,000-m^2 polygons shown in Extended Data Fig. 7. In this example, the lower discharge bound (red symbol) for the threshold shear stress model is defined as the lowest discharge for which modelled shear stresses exceed the lower shear stress threshold for sliding. The high discharge bound (blue symbol) is defined as the lowest discharge with modelled shear stresses that exceed the upper shear stress threshold for sliding.
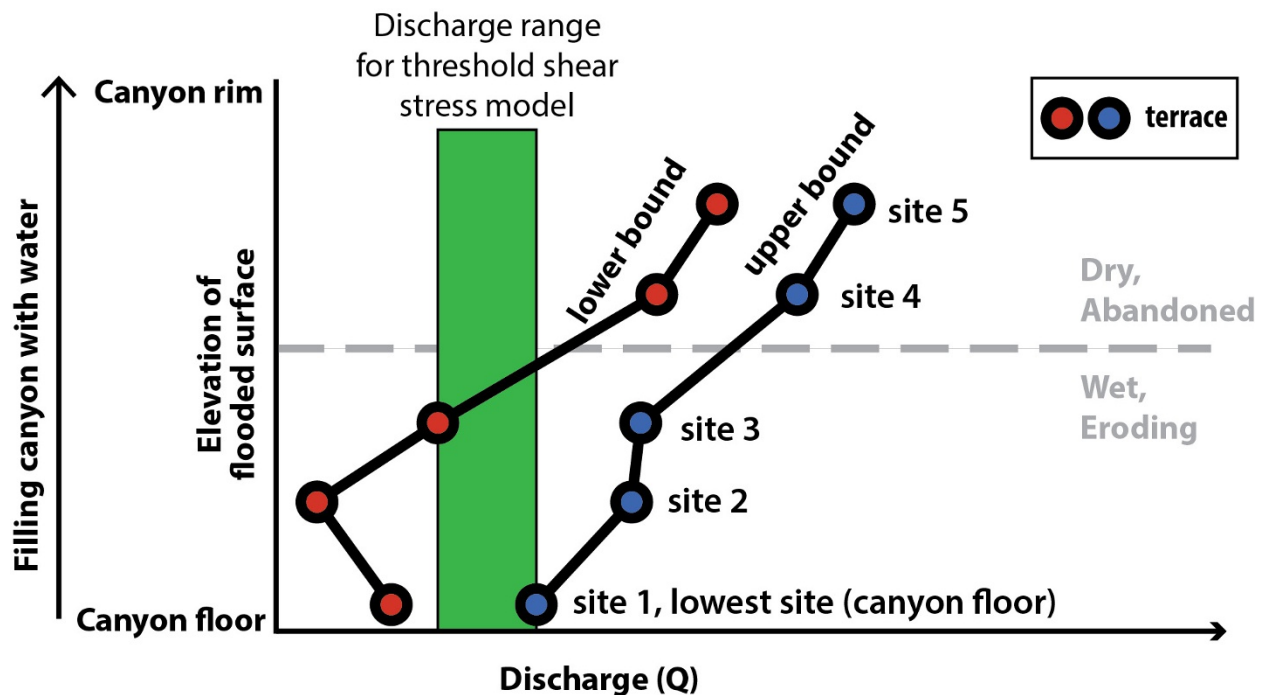
Extended Data Figure 9 | Schematic illustrating the method for defining the discharge range predicted by the threshold shear stress model. For a given topographic reconstruction we first used the upper and lower bed stress thresholds for block plucking via sliding to define the range of possible discharges that are consistent with the threshold stress model at the lowest elevation site (Extended Data Fig. 7). The lowest elevation was always the canyon floor. We then followed the same procedure to determine the discharge range at sites with progressively higher elevations (for example, sites 2–5) that produced bed stress that were within the bounds for plucking at the site of interest and for all lower elevation sites. The range of discharges determined by these two criteria is shown by the green box. These two criteria are important because, for a flood discharge to be consistent with the threshold shear stress model, all sites that are inundated and eroding, from the canyon floor upward, must have bed stresses that are within the bounds for plucking. If the discharge required to pluck blocks at a higher elevation site exceed that of a lower elevation site, then the higher sites were considered to be dry and abandoned and so were not used to define the range of discharges for that stage of canyon incision.
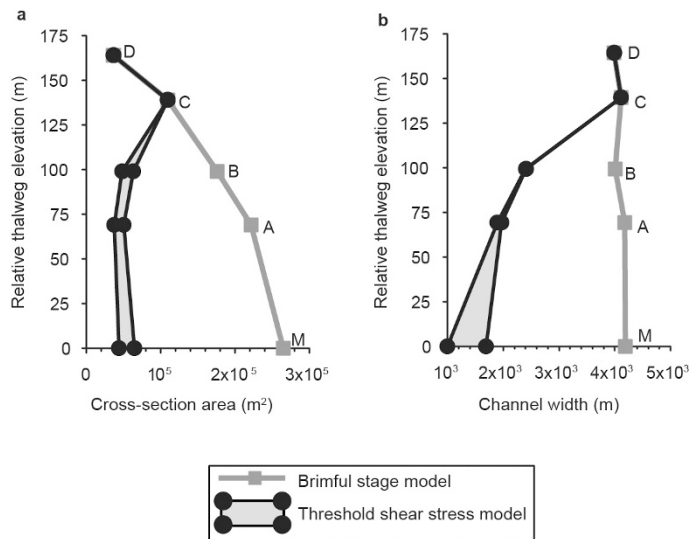
Extended Data Figure 10 | Predicted channel cross-sectional areas and widths. a, **b**, Cross-sectional area (**a**) and channel width (**b**) predicted by the brim-full model and threshold shear stress model. The shading shows the range of predicted values based on upper- and lower-bound parameterizations of the critical dimensionless shear stress for bedrock incision by block sliding (see Methods). For the initial topography (bed elevation D), where basalt is primarily overlain by loess, modelled shear stresses are lower than the threshold for plucking. At bed elevation C, modelled shear stresses at brim-full discharge are within 5% of the lower threshold for plucking; hence, bed stresses are assumed to be sufficient for plucking when flow was brim-full. For all other bed topographies, brim-full discharge greatly exceeds predicted values for plucking and sediment initial motion. The letters A–D denote simulation results for bed elevations A–D; M denotes results for the modern topography.